Title
Hydration water mobility is enhanced around tau amyloid fibers

Journal
Proceedings of the National Academy of Sciences of the United States of America, 112(20)

ISSN
0027-8424

Authors
Fichou, Yann
Schirò, Giorgio
Gallat, François-Xavier
et al.

Publication Date
2015-05-19

DOI
10.1073/pnas.1422824112

Hydration water mobility is enhanced around tau amyloid fibers

Yann Fichou[a,b,c,1], Giorgio Schirò[a,b,c], François-Xavier Gallat[a,b,c], Cedric Laguri[a,b,c], Martine Moulin[d], Jérôme Combet[e,f], Michaela Zamponi[g], Michael Härtlein[d], Catherine Picart[h,i], Estelle Mossou[d,j], Hugues Lortat-Jacob[a,b,c], Jacques-Philippe Colletier[a,b,c], Douglas J. Tobias[k,1], and Martin Weik[a,b,c,1]

[a]Université Grenoble Alpes, [b]CNRS, and [c]Commissariat à l'Énergie Atomique et aux Énergies Alternatives, Institut de Biologie Structurale, 38044 Grenoble, France; [d]Life Sciences Group, Institut Laue-Langevin, 38000 Grenoble, France; [e]Institut Laue Langevin, 38000 Grenoble, France; [f]Institut Charles Sadron CNRS–UdS, 67034 Strasbourg, France; [g]Jülich Centre for Neutron Science, outstation at Heinz Maier-Leibnitz Zentrum, Forschungszentrum Jülich GmbH, 85747 Garching, Germany; [h]CNRS, UMR 5628, LMGP, 38016 Grenoble, France; [i]Université de Grenoble Alpes, Grenoble Institute of Technology, 38016 Grenoble, France; [j]Faculty of Natural Sciences, Keele University, Staffordshire ST5 5BG, United Kingdom; and [k]Department of Chemistry, University of California, Irvine, CA 92697-2025

Edited by Michael L. Klein, Temple University, Philadelphia, PA, and approved March 27, 2015 (received for review December 1, 2014)

The paired helical filaments (PHF) formed by the intrinsically disordered human protein tau are one of the pathological hallmarks of Alzheimer disease. PHF are fibers of amyloid nature that are composed of a rigid core and an unstructured fuzzy coat. The mechanisms of fiber formation, in particular the role that hydration water might play, remain poorly understood. We combined protein deuteration, neutron scattering, and all-atom molecular dynamics simulations to study the dynamics of hydration water at the surface of fibers formed by the full-length human protein htau40. In comparison with monomeric tau, hydration water on the surface of tau fibers is more mobile, as evidenced by an increased fraction of translationally diffusing water molecules, a higher diffusion coefficient, and increased mean-squared displacements in neutron scattering experiments. Fibers formed by the hexapeptide ^{306}VQIVYK^{311} were taken as a model for the tau fiber core and studied by molecular dynamics simulations, revealing that hydration water dynamics around the core domain is significantly reduced after fiber formation. Thus, an increase in water dynamics around the fuzzy coat is proposed to be at the origin of the experimentally observed increase in hydration water dynamics around the entire tau fiber. The observed increase in hydration water dynamics is suggested to promote fiber formation through entropic effects. Detection of the enhanced hydration water mobility around tau fibers is conjectured to potentially contribute to the early diagnosis of Alzheimer patients by diffusion MRI.

hydration water | tau protein | amyloid fibers | intrinsically disordered proteins | neutron scattering

Amyloid fibers are the most stable forms of ordered protein aggregates. They have attracted much attention because of their implication in so-called conformational diseases, which include a variety of neurodegenerative disorders (1). Consequently, means of hindering or reversing fiber formation are actively researched (2). Pathological fibers are often formed by intrinsically disordered proteins (IDPs) that lack a well-defined 3D structure in their native state and are best described by an ensemble of different conformations (3). The human protein tau is an IDP that normally regulates microtubule stability in neurons. When tau aggregates, it forms paired helical filaments (PHF) that are one of the two histological hallmarks of Alzheimer disease (AD) (4, 5). As yet, and despite considerable effort over the past 30 y, the understanding of tau fibrillation in AD and other taupathies remains largely incomplete (6). The longest human tau isoform, htau40, is composed of 441 amino acid residues and is organized into several domains (see Fig. 1), including the repeat domains R1–R4 (residues 244–369) that constitute, together with the P1 and P2 domains, the microtubule binding regions (7). Essential for the nucleation of tau fibers is the presence of hexapeptides (^{275}VQIINK^{280} and ^{306}VQIVYK^{311}) in R2 and R3 (8) that have a high propensity to form β-structures. Although precise structures of tau PHF remain unknown (6), they can be divided into two structurally different regions (see Fig. 1): (*i*) a rigid β-rich core (denoted as the fiber core domain), which is essentially composed of the four repeat domains, and (*ii*) the remainder, the so-called fuzzy coat, which is highly flexible (9–11).

Water is known to play key roles in protein folding, stability, and activity (12). It mediates protein–protein and protein–DNA recognition, is involved in allostery, partakes in enzymatic reactions and proton and electron transfer, and more generally plasticizes biological macromolecules by providing their surface with an extensive and highly dynamic network of hydrogen bonds. Compared with folded proteins, tau has been shown to have a stronger coupling with its hydration water (13). However, very little is known about the role water plays in protein aggregation in general and in tau fibrillation in particular. A recent study on two different amyloid systems concluded that water plays a key role in fiber growth and polymorphism, *inter alia* through entropic effects (14). A study by Chong and Ham (15) highlighted the role of water in protein aggregation propensity by revealing a tight relation between the hydration free energy of a protein and its propensity to aggregate.

Among the experimental methodologies available to study protein hydration water, neutron scattering (NS) stands out owing to its pronounced sensitivity to motions of hydrogen atoms. Indeed, hydrogen atoms incoherently scatter neutrons about two

Significance

Protein aggregation into amyloid fibers and oligomers is observed in a variety of neurodegenerative diseases. The fibers formed by the intrinsically disordered human protein tau, for instance, are one of the hallmarks of Alzheimer disease. In this work, we report on the dynamic behavior of tau hydration water, which we found to be more mobile in tau fibers than in nonaggregated tau. This increase in mobility could promote fiber formation through an increase in hydration water entropy. That hydration water is more mobile around the pathological form of tau corroborates that methodologies sensitive to the diffusion of water, such as diffusion magnetic resonance imaging, could be used to diagnose Alzheimer patients in an early stage of the disease.

Author contributions: Y.F., J.-P.C., and M.W. designed research; Y.F., F.-X.G., J.C., M.Z., C.P., E.M., J.-P.C., and D.J.T. performed research; C.L., M.M., M.H., and H.L.-J. contributed new reagents/analytic tools; Y.F. and G.S. analyzed data; and Y.F., G.S., and M.W. wrote the paper with input from all authors.

The authors declare no conflict of interest.

This article is a PNAS Direct Submission.

Freely available online through the PNAS open access option.

[1]To whom correspondence may be addressed. Email: martin.weik@ibs.fr, yann.fichou@ibs.fr, or dtobias@uci.edu.

This article contains supporting information online at www.pnas.org/lookup/suppl/doi:10.1073/pnas.1422824112/-/DCSupplemental.

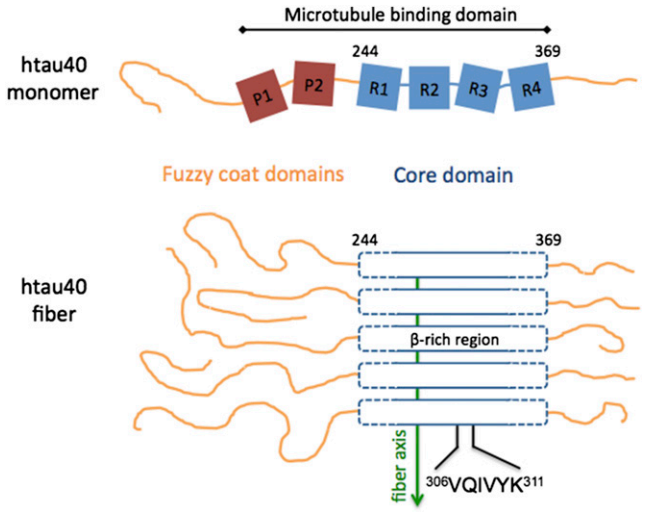

Fig. 1. Schematic representation of the tau isoform htau40 in its monomeric (*Top*) and fibrillated (*Bottom*) forms. The microtubule binding domain is roughly composed of the four repeat domains R1–R4 (residues 244–369) and the proline-rich domains P1 and P2. R1–R4 constitute the core domain, which forms cross-β structures as well as steric zippers in the fiber, whereas the rest of the protein is referred to as the fuzzy coat domain, which remains disordered in the fiber form. The amyloidogenic hexapeptide ^{306}VQIVYK^{311} can be used as a model for the fiber core.

orders of magnitude more strongly than all other atoms present in a biological sample, including deuterium atoms. Consequently, NS has been widely used to study bulk and confined water at room temperature (16), hydration water of peptides (17), proteins (18–21), and water inside cells (22). More specifically, NS probes atomic motions on the nanosecond to picosecond timescales and on the angstrom length scales (23), thus ensuring the time and space resolution necessary for investigating water dynamics with atomistic detail. Elastic incoherent NS (EINS) reflects the global dynamics averaged over all atoms but does not provide any information on the nature of the observed motions. Quasi-elastic NS (QENS), however, allows the quantification of energy exchanges between the sample and the neutron beam and provides quantitative information about the nature of motions observed. Because of a pronounced isotope effect, the replacement of hydrogen by deuterium atoms effectively masks the labeled part of a sample in incoherent NS experiments. Perdeuteration of proteins (i.e., deuteration of the entire protein) hydrated in H_2O thus puts the focus on hydration water dynamics by minimizing the protein contribution to the NS signal. All-atom molecular dynamics (MD) simulation is a useful complement to NS because both methods probe atomic motions on the same time and length scales. Whereas incoherent NS provides an accurate measure of the average dynamics of hydrogen atoms throughout the sample, MD simulations provide atomic-scale insight into motions occurring within particular space and time windows of interest (24).

Here we experimentally and computationally address the effect of tau fiber formation on the dynamics of its surrounding hydration water. We produced perdeuterated htau40 as well as a perdeuterated heparin analog, and measured by NS the dynamical properties of hydration water on the surface of tau monomers and of tau fibers whose formation was triggered by the heparin analog. Both elastic and quasi-elastic NS indicate an increased mobility of hydration water on tau fibers compared with tau monomers. MD simulations provide circumstantial evidence suggesting that it is the increase in water dynamics around the disordered fuzzy coat and not around the fiber core that is at the origin of the experimentally observed increase in tau hydration water dynamics after fibrillation. We conjecture that the observed gain in water dynamics reflects an increase in water entropy that is favorable to the fiber formation.

Results

Tau Fiber Characterization. Fibers formed by adding heparin to monomeric tau have been reported to closely resemble those formed in vivo by tau hyperphosphorylation in AD brains (25). Here we produced and used deuterated versions of tau and heparin to largely mask their incoherent contribution in NS experiments and thus focus on the hydration water dynamics around tau fibers. To exclude an isotope effect on fiber formation and morphology, we characterized deuterated fibers by complementary biophysical methods. A negative staining electron micrograph of the deuterated tau fibers is presented in Fig. 2*A*. Control micrographs of the monomeric tau did not reveal the presence of fibers. X-ray fiber diffraction patterns of deuterated tau fibers (Fig. 2*B*) showed the typical signature of amyloid structures. The diffraction ring at 4.7 Å corresponds to the cross-β sheet distance along the fiber direction, and the ring at 9 Å reflects the gauge of the steric zipper, perpendicular to the fiber direction (26, 27). Similar observations were made on hydrogenated tau fibers and monomers as shown in Fig. S1. We conclude that adding deuterated heparin to monomeric deuterated htau40 leads to the formation of fibers resembling those formed from hydrogenated constituents.

Water Mean-Squared Displacements Are Increased at the Surface of Tau Fibers. We performed EINS on powders of fibers (denoted as D-fiber-H_2O) and monomers (D-tau-H_2O) of deuterated tau hydrated at 0.4 g H_2O/g protein. This experiment aimed at measuring the dynamics of the first hydration shell of the protein in both states. Hydrogen atoms in the hydration water contribute 71% to the incoherent NS signal in both samples, whereas the remainder originates from the deuterated proteins, including exchanged hydrogen atoms (see *SI Materials and Methods* for detailed calculations). The contribution of deuterated heparin potentially included in the fibers is negligible (see *SI Materials and Methods*). Incoherent NS experiments from D-fiber-H_2O and D-tau-H_2O thus mainly monitor hydration water dynamics. Mean-squared displacements (MSD) of hydration water in both samples were extracted by applying a Gaussian approximation (see *SI Materials and Methods* for details), and are presented as a function of temperature in Fig. 3*A*. The MSD of D-fiber-H_2O become markedly larger than those of D-tau-H_2O above around 220 K, where large-amplitude water motions set in (28). At 300 K, they are about 30% higher for the fiber compared with the monomer sample. Hydration water is thus more mobile around the tau fibers than around the monomeric protein. The total elastically scattered intensity, which provides a model-free estimation of the dynamics, confirms the difference seen in the water MSD between D-fiber-H_2O and D-tau-H_2O (Fig. S2*A*).

Water Translational Diffusion Is Increased Around Tau Fibers. To provide quantitative information about the nature of water motions observed, we recorded QENS spectra on the D-fiber-H_2O and D-tau-H_2O samples at 280 K. The raw spectra are shown in Fig. 3*B*. The D-fiber-H_2O spectrum exhibits a larger quasi-elastic broadening, confirming qualitatively the enhanced dynamics of

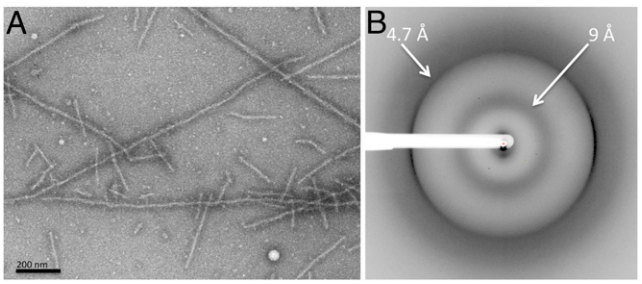

Fig. 2. (*A*) Electron micrograph and (*B*) X-ray fiber diffraction pattern of deuterated tau amyloid fibers. The white arrows highlight the diffraction rings observed at 4.7 Å and 9.0 Å, which are characteristic of amyloid structures.

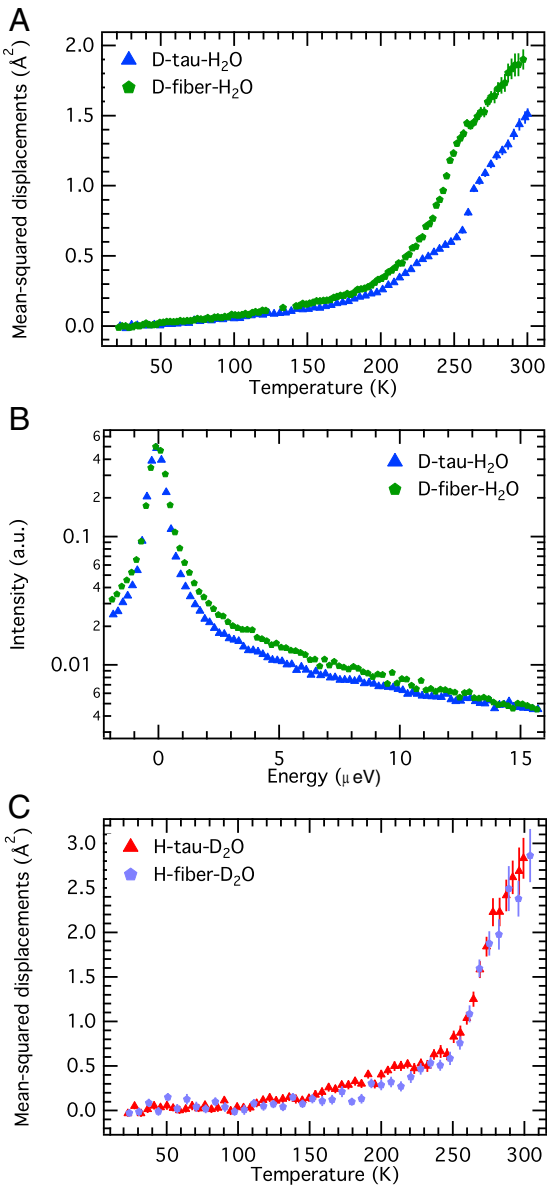

Fig. 3. (*A*) MSD of the hydration water around monomers (D-tau-H_2O) and fibers (D-fiber-H_2O) of the tau protein. The MSD were extracted from the Gaussian approximation fitted between q values of 0.78 Å^{-1} and 1.76 Å^{-1}. (*B*) Comparison of the raw QENS spectra of D-fiber-H_2O and D-tau-H_2O at 280 K, binned over q values from 0.45 Å^{-1} to 1.66 Å^{-1}. The spectra of D-tau-H_2O were extracted from Schiró et al. (29). For a visual comparison, the spectra were scaled with a multiplicative factor and corrected for a linear background. Because QENS spectra are symmetrical, the focus was put on positive energy exchange. (*C*) MSD of monomers (H-tau-D_2O) and fibers (H-fiber-D_2O) of the tau protein. They were extracted from the Gaussian approximation with a q^4 correction between q values of 0.43 Å^{-1} and 1.93 Å^{-1}. The error bars represent the SD output from the fitting procedure. Data on H-tau-D_2O were taken from ref. 13 and reanalyzed.

fiber hydration water evidenced by the MSD (Fig. 3*A*). QENS data were fitted with a model (29) that describes water diffusional dynamics as a superposition of translational and rotational motions, with a supplementary term for immobile water molecules (see *SI Materials and Methods* for details and Fig. S3 for an example of fits). The fitting procedure allows extraction of the fraction of the scattering signal coming from translating, rotating, or immobile water molecules, as well as their respective diffusion coefficients. Table S1 presents the output parameters of the fitting procedure. The fraction of water molecules undergoing translational diffusion around the fibers is 25% higher than around the monomers. Furthermore, the translational diffusion coefficient and the rotational rate are 11% and 17% higher, respectively, for the fiber hydration water.

Protein Dynamics of Tau Monomers and Fibers Are Identical. To determine if the enhancement of hydration water dynamics originates from a change in protein dynamics upon fibrillation, we measured by EINS the dynamics of the fibrillated and the monomeric tau protein. To this end, we prepared hydrogenated tau amyloid fibers, hydrated with 0.4 g D_2O per gram of protein (H-fiber-D_2O), strictly following the protocol established for formation of the D-fibers. Incoherent NS from such a sample amounts to 97% from the protein and only 3% from the hydrating D_2O (detailed calculations are presented in *SI Materials and Methods*) and, hence, almost solely reflects protein dynamics, and not water dynamics. We extracted the MSD (Fig. 3*C*) of tau fibers (H-fiber-D_2O) and compared them to those of monomeric tau [H-tau-D_2O; reprocessed from Gallat et al. (13)]. We applied a q^4 correction to the Gaussian approximation (see Fig. S4 and *SI Materials and Methods* for details) that allows fitting a large q range and provides not only the MSD but also the width of the MSD distribution (30, 31). This width reflects the heterogeneity of the MSD among the various hydrogen atoms in the protein. Note that this model was not suitable to fit scattering data from the deuterated samples. The H-fiber-D_2O and H-tau-D_2O samples present identical MSD (Fig. 3*C*) with similar distributions (Fig. S5). Thus, both tau monomers and fibers exhibit the same protein dynamics on the nanosecond to picosecond timescales, and the differences in water dynamics are inherent to the hydration shell.

MD Simulation Shows Decreased Water Dynamics Around the Fibrillated Hexapeptide ^{306}VQIVYK^{311}. The structure of tau fibers is heterogeneous in the sense that about 30% of the monomer is included in a cross-β structure (referred as the fiber core), whereas the rest remains disordered (fuzzy coat; see Fig. 1). Because NS provides information on the average dynamics of all hydrogen atoms in the sample, we used MD simulations to assist the interpretation of our experimental results (see *Discussion*). We carried out all-atom MD simulations on the amyloid-prone hexapeptide ^{306}VQIVYK^{311}, which belongs to the tau fiber core (8) and was therefore used as a model of the fiber core (32, 33). The simulation was performed on the monomeric peptide in solution (Fig. S6*A*) and the peptide fiber based on the crystal structure (34) [Protein Data Bank (PDB) entry 2ON9; Fig. S6*B*], following the procedure described by Zhao et al. in ref. 35. We compared the dynamics of the water molecules (Fig. 4) around the monomeric peptide (highlighted in Fig. S6*A*) and around the peptide fiber (highlighted in Fig. S6*B*). The MSD of hydration water (Fig. 4*A*) are higher for the monomeric compared with the fibrillated peptide. To provide further insight into water behavior at the surface of the peptide, two types of peptide–water hydrogen bond (HB) correlation functions were analyzed: the continuous HB correlation function, the decay of which defines the timescale, on average, on which protein–water HBs break, and the intermittent HB correlation function, the decay of which defines the timescale of the rearrangement of the protein–water HB network. The decay of the continuous HB correlation function is due primarily to the rotational/librational motions of water molecules, whereas the decay of the intermittent HB correlation function results from the reorganization of the protein HB network due to water translational diffusion (36). The relaxation times of both correlation functions are longer (Fig. 4 *B* and *C*) when the peptide is in the amyloid state, suggesting, consistently with the water MSD (Fig. 4*A*), that the hydration water dynamics around the core domain is slowed down after fiber formation.

Discussion

The mobility of hydration water on the surface of tau fibers is increased compared with tau monomers as evidenced by elastic

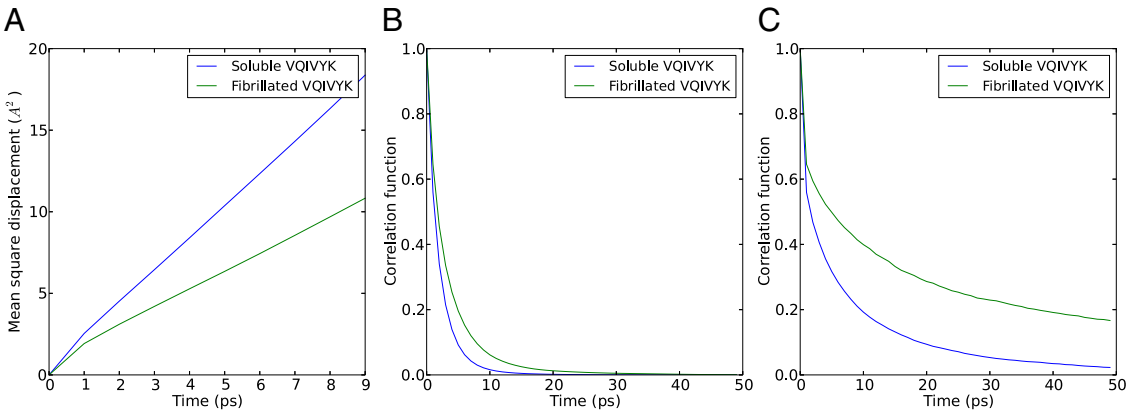

Fig. 4. Dynamical properties of the hydration water around the fibrillated and the monomeric peptide ^{306}VQIVYK^{311}, obtained by MD simulations. (*A*) MSD of the first hydration shell (defined as water molecules within 3 Å of the peptide), (*B*) protein–water continuous HB correlation function (providing information on the timescale of water rotational/librational dynamics), and (*C*) protein–water intermittent HB correlation function (providing information on the timescale of the rearrangement of the protein–water HB network due to water translational diffusion).

and quasi-elastic NS. Quantitatively, 25% more water molecules undergo translational diffusion on the fiber surface, and they display an 11% higher diffusion coefficient. The protein dynamics of monomeric and fibrillar tau appear to be identical, implying that the observed differences in water dynamics are inherent to the hydration shell. MD simulation, carried out on a model of the fiber core, shows a reduced water mobility around the amyloid form of the fiber core model.

Is the experimentally observed average increase in hydration water dynamics around fibrillar tau due to enhanced dynamics of water around the core or the fuzzy coat domains (see Fig. 1 for a visual representation of these domains)? To address this question, we divide the average hydration water dynamics in two parts (see Fig. 1): the dynamics of the water molecules around residues 244–369 (forming the core domain in the fibers) and around residues 1–243 and 370–441 (forming the fuzzy coat in the fibers). The subscripts *core* and *fuzz* refer to these two groups, respectively, and the subscript *tot* refers to the water around the entire protein. Note that the definition of these groups applies to both the monomeric and the fibrillated protein. Then, one can write

$$\langle u\rangle_{tot} = p_{fuzz} \times \langle u\rangle_{fuzz} + p_{core} \times \langle u\rangle_{core}, \qquad [1]$$

where $\langle u\rangle$ are the mean values of a generic dynamic parameter, and p_{fuzz} and p_{core} are fractions of water molecules at the surface of the fuzzy coat and the core domain, respectively, with $p_{fuzz} + p_{core} = 1$. Note that u represents any dynamical quantity, such as MSD, for instance. Following Eq. **1**, our experimental finding can be written as $\langle u\rangle_{tot}^{fib} > \langle u\rangle_{tot}^{mon}$, where the superscripts *fib* and *mon* refer to the fibrillated and monomeric protein, respectively.

During tau fibrillation, a fraction of the core domain becomes dehydrated when it forms dry steric zippers (34) and cross-β sheets, i.e., $p_{core}^{fib} < p_{core}^{mon}$ and thus $p_{fuzz}^{fib} > p_{fuzz}^{mon}$. If the average amino acid composition of core and fuzzy coat were markedly different, in particular resulting in a different hydrophobicity, a redistribution of water from the core to the fuzzy coat after fibrillation could affect hydration water dynamics (17, 37). However, according to the hydropathy scale of Kyle and Doolittle (38), the average hydropathy of the core and fuzzy coat are similar (-0.6 ± 1.3 and -0.9 ± 1.4, respectively). This similarity thus suggests that $\langle u\rangle_{fuzz}^{mon} \approx \langle u\rangle_{core}^{mon}$ and that a redistribution of water between core and fuzzy coat domains is not at the origin of the experimentally observed increase in the average tau hydration dynamics after fibrillation.

Another possible origin of the enhanced hydration water dynamics observed on the surface of tau fibers is an increase in water dynamics on the core moiety after fiber formation. The amyloid core is composed of β-sheets that are stabilized by intermolecular HBs, thus reducing the number of HB donors and acceptors available for interaction with hydration water. As a consequence, one could conjecture that water moves more freely on the fiber core, thus leading to $\langle u\rangle_{core}^{fib} > \langle u\rangle_{core}^{mon}$. To evaluate this possibility in silico, we chose the hexapeptide ^{306}VQIVYK^{311} as a model for the fiber core and carried out MD simulations of both monomeric and amyloid fiber states. The analysis of water dynamics in the first hydration layer shows an overall lower mobility around the amyloid form, as revealed by water total MSD (see Fig. 4*A*). In particular, both the continuous (Fig. 4*B*) and the intermittent (Fig. 4*C*) protein–water HB relaxation times are longer around the fibrillated peptides, suggesting that both rotational and translational diffusions are reduced around the amyloid assembly. A reduction in the local dynamics of water molecules around the core domain in tau fibers (in particular around the residue Cys322) has also been observed in Overhauser dynamic nuclear polarization NMR experiments (39). Therefore, we propose that it is the water dynamics not around the core domain but around the fuzzy coat that is increased when tau has formed amyloid fibers, resulting in the average increase in water dynamics observed in our neutron experiments. Spatially resolved water dynamics on the core and on the fuzzy domains could be monitored with time-resolved fluorescence lifetime measurements (40).

The local protein topology, determined by the protein conformation, has been proposed to be a key, if not the main, feature determining the hydration water dynamics (41–44). Significant conformational changes in the fuzzy coat have been shown by NMR spectroscopy to accompany tau fiber formation (11); thus a change in water mobility upon fiber formation is expected. A rough model of a tau fiber has been proposed based on EM and atomic force microscopy experiments, in which the fuzzy coat resembles a two-layered polyelectrolyte brush with the protein termini sticking out of the fiber core (45). In view of this model, one might conjecture that the alignment of the protein termini within the fuzzy coat after fiber formation modifies the confinement geometry of hydration water. In particular, the confinement dimensionality might be reduced from 3D before to 1D or 2D after fiber formation, thus increasing water mobility, as shown in model systems by, e.g., MD simulations and experiments (46, 47). Thus, we propose that the conformational change of the fuzzy coat imposed by formation of the fiber core is responsible for the experimentally observed increase in water dynamics.

A macromolecular surface perturbs hydration water with respect to bulk water, resulting in a decrease in both water dynamics and water entropy. The notion of water being a reservoir of entropy for biomolecules has been discussed in the context of protein folding, binding, and aggregation (14, 48–50). Energetically

unfavorable protein conformational changes can feed upon the water entropy. For instance, Breiten et al. showed experimentally that water entropy compensates for the poor binding enthalpy of a protein–ligand complex (49). Several studies (14, 51) have shown that the nucleation of amyloid structures requires surmounting a free energy barrier. That this thermodynamic cost can be compensated by an increase in hydration entropy through the release of water into the bulk has been shown in silico (14). Our observed increase in the fraction of water molecules undergoing translational diffusion on the fiber surface reflects a decrease in water perturbation and thus a gain in water entropy. A tentative estimation of the entropy gain associated with the addition of water translational degrees of freedom could be based on the increase in the number of translating water molecules around tau fibers (see Table S1). However, it has been shown (see, e.g., ref. 52) that the translational entropy of a water molecule interacting with a protein depends not only on the surface hydrophobicity but also largely on the water–protein distance. Consequently, without knowing the surface topology of tau fibers at high resolution, any quantitative estimation of the entropy change would not be reliable. Nevertheless, from a qualitative point of view, we propose that the entropy gain associated with the increase in the number of translating water molecules promotes fiber formation.

Many studies have examined fibers formed only by the core domains (so-called K18 and K19 fragments) as models for the biologically relevant tau PHF. Our work provides an example of a property that differs significantly between the fiber core domain (reduced hydration dynamics) and the full-length tau fibers (enhanced hydration water dynamics). Care should thus be taken when extrapolating experimental results obtained on a protein fragment fiber to a full-length protein fiber.

An increase in water diffusivity has been observed with diffusion MRI in the hippocampus of patients suffering from AD (53, 54) and proposed as a potential early biomarker of the disease. This increase has been hypothesized to originate from the decrease in neuronal cell density accompanying the progression of AD, yet experimental validation remains elusive. Our study raises the possibility that the enhanced water mobility around tau PHF could provide an additional explanation for the increased water diffusivity revealed by diffusion MRI. Indeed, although the local density of PHF within volumes of brains corresponding to the spatial resolution of MRI [~1 mm^3 (55)] remains unknown to the best of our knowledge, PHF have been shown to be densely packed within neuronal cells (see, e.g., figure 4 in ref. 56), and the proportion of accelerated PHF hydration water compared with bulk-like water might thus be substantial. In addition, islands of dystrophic neurons containing PHF in AD-affected brains have been shown to reach 1 mm in size (57). Consequently, accelerated PHF hydration water might well be at the origin, at least partially, of the enhanced water diffusivity in AD-affected brains detected by diffusion MRI.

In conclusion, we have provided experimental evidence for an increased hydration water mobility of tau fibers compared with monomers, which we tentatively assigned to an increase of water dynamics on the surface of the fuzzy coat. The ensemble of results presented suggests a scenario in which the hydration water mobility plays a role in the formation of tau amyloid fibers by providing entropic compensation. It would be highly interesting to follow water dynamics during the fibrillation process. The question of whether or not the growth rate of amyloid fibers can be modulated by acting on the solvent dynamics remains to be studied. If this were the case, efforts to mitigate the formation of tau amyloid fibers in the context of AD should be extended to include a focus on hydration water dynamics.

Materials and Methods

Expression, Purification, Fibrillation, and Sample Preparation of htau40 for Neutron Experiments. The expression and purification of the human isoform htau40 has been published elsewhere (13) and is briefly recalled in *SI Materials and Methods*. The deuterated fibers (denoted as D-fiber) and hydrogenated fibers (H-fiber) were prepared identically. The purified protein was mixed with the deuterated heparin analog (the production of which is described in *SI Materials and Methods*) at a molar ratio tau:heparin 4:1 to trigger fibrillation. The fibrillation was monitored by fluorescence of thioflavin S on a BioTek Synergy H4 Hybrid microplate reader with excitation and emission wavelengths of 430 nm and 490 nm, respectively. A typical fluorescence curve as a function of time of the hydrogenated protein solution is shown in Fig. S7.

After adding the deuterated heparin analog, the solutions were incubated at room temperature for the hydrogenated protein and at 30 °C for the perdeuterated protein for about 2 wk. The fibers were then extracted by centrifugation at 125,000 g for 90 min and used for neutron sample preparation, as well as for biophysical characterization (see *SI Materials and Methods*). After lyophilization, the deuterated fibers were rehydrated to 0.40 g H_2O per gram of protein (sample denoted D-fiber-H_2O) and the hydrogenated fibers were rehydrated to 0.44 g D_2O per gram of protein (H-fiber-D_2O). Both samples were then sealed in a 4 × 3 cm^2 flat aluminum sample holder. A detailed protocol of the sample preparation is given in *SI Materials and Methods*. The deuterated and hydrogenated monomeric tau samples (i.e., D-tau-H_2O and H-tau-D_2O, respectively) were prepared previously (13).

EINS Experiments. EINS of D-fiber-H_2O and D-tau-H_2O was carried out on the backscattering Spectrometer for High Energy Resolution (SPHERES) (58) (Jülich Centre for Neutron Science at the Heinz Maier-Leibnitz Zentrum Garching, Garching, Germany). The instrumental energy resolution of 0.65 μeV (full width at half-maximum) allowed motions faster than about 1 ns to be probed. The instrument uses neutrons with a wavelength of 6.27 Å and scattering vectors q in the range of 0.21–1.84 $Å^{-1}$. EINS of H-fiber-D_2O was carried out on the backscattering spectrometer IN16 (59) at the Institut Laue Langevin (Grenoble, France). The instrumental energy resolution of 0.9 μeV (full width at half-maximum) allowed motions faster than about 1 ns to be probed. The instrument uses neutrons with a wavelength of 6.27 Å and scattering vectors q in the range of 0.19–1.95 $Å^{-1}$. Data on H-tau-D_2O, also measured on IN16, were taken from previous work (13) and reprocessed. The MSD were calculated using the Gaussian approximation (*SI Materials and Methods*).

QENS. QENS experiments on the D-fiber-H_2O sample were carried out on SPHERES (58). The data were collected over an energy range of −15.8/+15.6 μeV at 20 K and 280 K, for 10 h and 12 h, respectively. The spectra at 280 K (Fig. 3*B* and Fig. S3) were normalized to the 20-K spectra. QENS data on D-tau-H_2O, measured on SPHERES according to the same protocol, were obtained by Schiró et al. (29). Details on data processing and modeling are available in *SI Materials and Methods*.

MD Simulation. The monomeric peptide model was built by placing the hexapeptide ^{306}VQIVYK^{311} in a box containing 9,253 water molecules and 1 chloride ion for electroneutrality (see a snapshot of the simulation box in Fig. S6*A*). The fiber model was based on the work of Zhao et al. (35). The fiber was made of the antiparallel two-sheet crystal structure published by Sawaya et al. (34) (PDB entry 2ON9). Five strands were stacked on top of each other with a distance of 4.7 Å (Fig. S6*B*) and placed in a box of 9,258 water molecules. After 18 ns of equilibration, the dynamical parameters shown in Fig. 4 were computed over 2 ns for water molecules within 3 Å of the protein surface (see Fig. S6). Details on the simulation protocol and the calculations of the dynamical parameters are given in *SI Materials and Methods*.

ACKNOWLEDGMENTS. We are grateful to Daphna Fenel [EM facility within the Grenoble Partnership for Structural Biology (PSB)] for having carried out EM experiments and to Denis Le Bihan for discussion on a potential implication of the present work in diffusion MRI. The authors acknowledge Matthias Heyden for providing MD simulation analysis programs. This work used the platforms of the Grenoble Instruct Center [Unité Mixte de Service 3518 Centre National de la Recherche Scientifique (CNRS)-Commissariat à l'Energie Atomique et aux Energies Alternatives (CEA)-Université Joseph Fourier (UJF)-European Molecular Biology Laboratory (EMBL)] with support from French Infrastructure for Integrated Structural Biology (FRISBI) (ANR-10-INSB-05-02) and Grenoble Alliance for Integrated Structural Cell Biology (GRAL) (ANR-10-LABX-49-01) within PSB. Financial support by CEA, CNRS, and UJF is acknowledged, as well as a grant from the Agence Nationale de la Recherche (Project ANR-11-BSV5-027) to M.W. This work has benefited from the activities of the Deuteration Laboratory (DLAB) consortium funded by the European Union under Contracts HPRI-2001-50065 and RII3-CT-2003-505925, and from UK Engineering and Physical Sciences Research Council (EPSRC)-funded activity within the Institut Laue Langevin EMBL DLAB under Grants GR/R99393/01 and EP/C015452/1. Support by the European Commission under the 7th Framework Programme through the Key Action: Strengthening

the European Research Area, Research Infrastructures is acknowledged [Contract 226507 (NMI3)]. Y.F. is grateful to the Fulbright Scholar Program, which provided support for his visit to University of California, Irvine to carry out the MD simulations.

1. Chiti F, Dobson CM (2006) Protein misfolding, functional amyloid, and human disease. *Annu Rev Biochem* 75(1):333–366.
2. Lednev IK (2014) Amyloid fibrils: The eighth wonder of the world in protein folding and aggregation. *Biophys J* 106(7):1433–1435.
3. Uversky VN, Oldfield CJ, Dunker AK (2008) Intrinsically disordered proteins in human diseases: Introducing the D2 concept. *Annu Rev Biophys* 37(1):215–246.
4. Brion JP, Couck AM, Passareiro E, Flament-Durand J (1985) Neurofibrillary tangles of Alzheimer's disease: An immunohistochemical study. *J Submicrosc Cytol* 17(1):89–96.
5. Kosik KS, Joachim CL, Selkoe DJ (1986) Microtubule-associated protein tau (tau) is a major antigenic component of paired helical filaments in Alzheimer disease. *Proc Natl Acad Sci USA* 83(11):4044–4048.
6. Mandelkow EM, Mandelkow E (2012) Biochemistry and cell biology of tau protein in neurofibrillary degeneration. *Cold Spring Harb Perspect Med* 2(7):a006247.
7. Amos LA (2004) Microtubule structure and its stabilisation. *Org Biomol Chem* 2(15): 2153–2160.
8. von Bergen M, et al. (2000) Assembly of τ protein into Alzheimer paired helical filaments depends on a local sequence motif ((306)VQIVYK(311)) forming β structure. *Proc Natl Acad Sci USA* 97(10):5129–5134.
9. Wischik CM, et al. (1988) Isolation of a fragment of tau derived from the core of the paired helical filament of Alzheimer disease. *Proc Natl Acad Sci USA* 85(12):4506–4510.
10. Crowther T, Goedert M, Wischik CM (1989) The repeat region of microtubule-associated protein tau forms part of the core of the paired helical filament of Alzheimer's disease. *Ann Med* 21(2):127–132.
11. Bibow S, et al. (2011) The dynamic structure of filamentous tau. *Angew Chem Int Ed Engl* 50(48):11520–11524.
12. Ball P (2008) Water as an active constituent in cell biology. *Chem Rev* 108(1):74–108.
13. Gallat F-X, et al. (2012) Dynamical coupling of intrinsically disordered proteins and their hydration water: Comparison with folded soluble and membrane proteins. *Biophys J* 103(1):129–136.
14. Thirumalai D, Reddy G, Straub JE (2012) Role of water in protein aggregation and amyloid polymorphism. *Acc Chem Res* 45(1):83–92.
15. Chong S-H, Ham S (2014) Interaction with the surrounding water plays a key role in determining the aggregation propensity of proteins. *Angew Chem Int Ed Engl* 53(15): 3961–3964.
16. Bellissent-Funel M, Chen SH, Zanotti J (1995) Single-particle dynamics of water molecules in confined space. *Phys Rev E Stat Phys Plasmas Fluids Relat Interdiscip Topics* 51(5):4558–4569.
17. Russo D, Hura G, Head-Gordon T (2004) Hydration dynamics near a model protein surface. *Biophys J* 86(3):1852–1862.
18. Bellissent-Funel M-C, Teixeira J, Bradley K-F, Chen SH (1992) Dynamics of hydration water in protein. *J Phys I* 2(6):995–1001.
19. Doster W, et al. (2010) Dynamical transition of protein-hydration water. *Phys Rev Lett* 104(9):098101.
20. Achterhold K, et al. (2011) Dynamical properties of the hydration shell of fully deuterated myoglobin. *Phys Rev E Stat Nonlin Soft Matter Phys* 84(4 Pt 1):041930.
21. Nickels JD, et al. (2012) Dynamics of protein and its hydration water: Neutron scattering studies on fully deuterated GFP. *Biophys J* 103(7):1566–1575.
22. Frolich A, et al. (2009) From shell to cell: Neutron scattering studies of biological water dynamics and coupling to activity. *Faraday Discuss* 141:117–30, and discussion (2009) 141:175–207.
23. Gabel F, et al. (2002) Protein dynamics studied by neutron scattering. *Q Rev Biophys* 35(4):327–367.
24. Bizzarri AR (2004) Neutron scattering and molecular dynamics simulation: A conjugate approach to investigate the dynamics of electron transfer proteins. *J Phys Condens Matter* 16(6):R83–R110.
25. Goedert M, et al. (1996) Assembly of microtubule-associated protein tau into Alzheimer-like filaments induced by sulphated glycosaminoglycans. *Nature* 383(6600): 550–553.
26. Astbury WT, Dickinson S, Bailey K (1935) The X-ray interpretation of denaturation and the structure of the seed globulins. *Biochem J* 29(10):2351–2360-1.
27. Sunde M, et al. (1997) Common core structure of amyloid fibrils by synchrotron X-ray diffraction. *J Mol Biol* 273(3):729–739.
28. Wood K, et al. (2008) Coincidence of dynamical transitions in a soluble protein and its hydration water: Direct measurements by neutron scattering and MD simulations. *J Am Chem Soc* 130(14):4586–4587.
29. Schiró G, et al. (2015) Translational diffusion of hydration water correlates with functional motions in folded and intrinsically disordered proteins, *Nat Commun* 6:6490.
30. Becker T, Smith JC (2003) Energy resolution and dynamical heterogeneity effects on elastic incoherent neutron scattering from molecular systems. *Phys Rev E Stat Nonlin Soft Matter Phys* 67(2 Pt 1):021904.
31. Yi Z, Miao Y, Baudry J, Jain N, Smith JC (2012) Derivation of mean-square displacements for protein dynamics from elastic incoherent neutron scattering. *J Phys Chem B* 116(16):5028–5036.
32. Sievers SA, et al. (2011) Structure-based design of non-natural amino-acid inhibitors of amyloid fibril formation. *Nature* 475(7354):96–100.
33. Berhanu WM, Masunov AE (2011) Can molecular dynamics simulations assist in design of specific inhibitors and imaging agents of amyloid aggregation? Structure, stability and free energy predictions for amyloid oligomers of VQIVYK, MVGGVV and LYQLEN. *J Mol Model* 17(10):2423–2442.
34. Sawaya MR, et al. (2007) Atomic structures of amyloid cross-β spines reveal varied steric zippers. *Nature* 447(7143):453–457.
35. Zhao J-H, et al. (2010) Molecular dynamics simulations to investigate the stability and aggregation behaviour of the amyloid-forming peptide VQIVYK from tau protein. *Mol Simul* 36(13):1013–1024.
36. Tarek M, Tobias DJ (2002) Role of protein-water hydrogen bond dynamics in the protein dynamical transition. *Phys Rev Lett* 88(13):138101.
37. Jana B, Pal S, Bagchi B (2008) Hydrogen bond breaking mechanism and water reorientational dynamics in the hydration layer of lysozyme. *J Phys Chem B* 112(30): 9112–9117.
38. Kyte J, Doolittle RF (1982) A simple method for displaying the hydropathic character of a protein. *J Mol Biol* 157(1):105–132.
39. Pavlova A, et al. (2009) Site-specific dynamic nuclear polarization of hydration water as a generally applicable approach to monitor protein aggregation. *Phys Chem Chem Phys* 11(31):6833–6839.
40. Zhang L, et al. (2007) Mapping hydration dynamics around a protein surface. *Proc Natl Acad Sci USA* 104(47):18461–18466.
41. Luise A, Falconi M, Desideri A (2000) Molecular dynamics simulation of solvated azurin: correlation between surface solvent accessibility and water residence times. *Proteins* 39(1):56–67.
42. Makarov VA, Andrews BK, Smith PE, Pettitt BM (2000) Residence times of water molecules in the hydration sites of myoglobin. *Biophys J* 79(6):2966–2974.
43. Sterpone F, Stirnemann G, Laage D (2012) Magnitude and molecular origin of water slowdown next to a protein. *J Am Chem Soc* 134(9):4116–4119.
44. Bagchi K, Roy S (2014) Sensitivity of water dynamics to biologically significant surfaces of monomeric insulin: Role of topology and electrostatic interactions. *J Phys Chem B* 118(14):3805–3813.
45. Wegmann S, Medalsy ID, Mandelkow E, Müller DJ (2013) The fuzzy coat of pathological human Tau fibrils is a two-layered polyelectrolyte brush. *Proc Natl Acad Sci USA* 110(4):E313–E321.
46. Swenson J, Bergman R, Longeville S, Howells WS (2001) Dynamics of 2D-water as studied by quasi-elastic neutron scattering and neutron resonance spin-echo. *Physica B* 301(1-2):28–34.
47. Hummer G, Rasaiah JC, Noworyta JP (2001) Water conduction through the hydrophobic channel of a carbon nanotube. *Nature* 414(6860):188–190.
48. Harano Y, Kinoshita M (2004) Large gain in translational entropy of water is a major driving force in protein folding. *Chem Phys Lett* 399(4-6):342–348.
49. Breiten B, et al. (2013) Water networks contribute to enthalpy/entropy compensation in protein-ligand binding. *J Am Chem Soc* 135(41):15579–15584.
50. Brovchenko I, Oleinikova A (2008) Which properties of a spanning network of hydration water enable biological functions? *ChemPhysChem* 9(18):2695–2702.
51. Nelson R, et al. (2005) Structure of the cross-beta spine of amyloid-like fibrils. *Nature* 435(7043):773–778.
52. Sasikala WD, Mukherjee A (2014) Single water entropy: Hydrophobic crossover and application to drug binding. *J Phys Chem B* 118(36):10553–10564.
53. Kantarci K, et al. (2005) DWI predicts future progression to Alzheimer disease in amnestic mild cognitive impairment. *Neurology* 64(5):902–904.
54. Nir TM, et al.; Alzheimer's Disease Neuroimaging Initiative (2013) Effectiveness of regional DTI measures in distinguishing Alzheimer's disease, MCI, and normal aging. *Neuroimage Clin* 3:180–195.
55. Le Bihan D, Johansen-Berg H (2012) Diffusion MRI at 25: Exploring brain tissue structure and function. *Neuroimage* 61(2):324–341.
56. Itoh Y, Amano N, Inoue M, Yagishita S (1997) Scanning electron microscopical study of the neurofibrillary tangles of Alzheimer's disease. *Acta Neuropathol* 94(1):78–86.
57. Braak H, Braak E (1991) Neuropathological stageing of Alzheimer-related changes. *Acta Neuropathol* 82(4):239–259.
58. Wuttke J, et al. (2012) SPHERES, Jülich's high-flux neutron backscattering spectrometer at FRM II. *Rev Sci Instrum* 83(7):075109.
59. Frick B, Gonzalez M (2001) Five years operation of the second generation backscattering spectrometer IN16—A retrospective, recent developments and plans. *Physica B* 301(1-2):8–19.